JOURNAL OF COMPUTATIONAL PHYSICS 39, 1–21 (1981)

Computational Aspects of the Random Choice Method for Shallow Water Equations

GUILLERMO MARSHALL * AND RAÚL MÉNDEZ

Department of Mathematics, University of California, Berkely, California 94720

Received May 3, 1979; revised September 24, 1979

A numerical solution of the Shallow Water Equations is presented. The construction of the solution is based on the Random Choice Method consisting in the solution of Riemann problems and sampling techniques. As an illustration the method is applied to the problem of the breaking of a dam. The main advantages of the method described lie in its ability to simulate discontinuities and in its lack of numerical dissipation.

1. INTRODUCTION AND GENERAL CONSIDERATIONS

The existence, in general, of discontinuities in the solution of non-linear hyperbolic partial differential equations is a well known fact. These discontinuities may be produced by non-smooth initial data or may very well develop spontaneously in the domain, even in the case of smooth initial data. The hyperbolic equations that we study here are mathematical statements of conservation laws and therefore integral relations the solutions of which need not be continuous. These solutions are called generalized solutions (weak solutions). Uniqueness is achieved when the non-linear hyperbolic system of conservation laws satisfies the Rankine–Hugoniot relations and the entropy condition, at the line of discontinuity, (see, for instance, Lax [7] or Chorin and Marsden [4]). In the solution of systems of quasi-linear hyperbolic equations in gas dynamics, discontinuities arise when shock waves, rarefaction waves, and slip lines are present. A typical example of this phenomenon is provided by the experiment of the shock tube problem in which two gases, initially at rest, with different pressures and densities and separated by a diaphragm, are brought in contact by the sudden destruction of the diaphragm; the higher pressure gas expands in the direction of the lower pressure gas, producing a shock and a slip line (travelling in the same direction), and a rarefaction wave (travelling in the opposite direction).

The hyperbolic quasi-linear system of equations governing the flow of an ideal incompressible fluid, in a gravitational field, with a free surface and when the depth of the fluid is considered small, is termed Shallow Water Equations. In the solution of

* Current address: Comisión Nacional de Energía Atómica, Centro de Cómputos, Avenida del Libertador 8250, 1429 Buenos Aires, Argentina.

0021-9991/81/010001-21$02.00/0

these equations discontinuities arise when bores or hydraulic jumps are present. A rather classical example of such a phenomenon is provided by the problem of the breaking of a dam (see, for instance, Stoker [12] or Strelkoff *et al.* [13]), in which two different surface levels of water initially at rest and separated by the dam are brought into contact by the sudden failure of the dam. The high level water flows in the direction of the low level water, producing a bore travelling in the same direction and a depression wave travelling in the opposite direction.

The formal similarity between the shock tube problem and the breaking of a dam is transparent. In fact, this similarity is supported by the well known analogy between the equations of the isoentropic flow of a perfect gas with constant specific heat and the shallow water equations. In both theories the analogy is greatly illuminated by the method of characteristics (see, for instance, Courant and Friedrichs [6], Stoker [12], or Abbott [1]). In the course of this study we extend results of gas dynamics to shallow water equations by virtue of that analogy.

In gas dynamics the presence of a compressive shock implies an increase of the entropy at the shock which is exclusively defined by the laws of conservation of mass, momentum and energy; the thickness of the shock depends on the dissipative mechanism process. In the shallow water analogy the situation bears some resemblance: through the hydraulic jump there is a loss of energy which depends on the laws of conservation of mass and momentum while the thickness of the jump depends on the dissipative mechanism, namely, turbulence. The theory of ideal gases or its hydraulic analogy cannot describe the mechanism of the discontinuity or its thickness; it can only represent the shock as an ideal curve with zero thickness. The similarity solutions provided by the two theories preclude any characteristic length which may serve as a scale of the thickness of the shock layer.

In the recent past considerable effort has been devoted to the improvement of the numerical solutions of one dimensional gas dynamic equations and its hydraulic analogy (see, for instance, Sod [10] and Strelkoff *et al.* [13]). Recently Chorin [2] introduced the Random Choice Method (RCM), which is based on an approximate method for the construction of solutions of non-linear hyperbolic systems of conservation laws developed by Glimm (see Lax [7]). In the RCM the solution is constructed as a superposition of locally theoretical solutions and sampling techniques. The main advantage of the RCM over other numerical methods lies in its lack of numerical dissipation and, for the case of hyperbolic systems with constant coefficients, in its infinite resolution.

The RCM has been applied to a wide variety of problems. Chorin [3] solved reacting gas flows and flame propagation; Sod [10, 11] made extensive comparisons of the RCM with other recent finite difference schemes and extended the RCM for radially and spherically symmetric gas dynamical flows; Concus and Proskurowski [5] solved a non-linear hyperbolic equation in porous media.

In the present work we outline the main aspects of the RCM for the shallow water equations in the light of the analogy with gas dynamics. Numerical results for the problem of the breaking of a dam are shown.

2. Single Conservation Laws and the Random Choice Method

We introduce briefly the main features of hyperbolic equations in conservation form ad a simple example of the application of the RCM. Consider the initial value problem

$$u_t + f(u)_x = 0, \tag{2.1}$$

where $f(u) = -au$ (a is a constant greater than zero); the initial conditions are

$$u(x, 0) = F(x). \tag{2.2}$$

The hyperbolic equation (2.1) is said to be written in conservation form and describes a single conservation law. Denote

$$a(u) = \frac{df(u)}{du} = -a. \tag{2.3}$$

Thus (2.1) can be written in the equivalent form

$$u_t - au_x = 0. \tag{2.4}$$

The theoretical solution of (2.1) or (2.4) is

$$u(x, t) = F(x + at). \tag{2.5}$$

The fact that $u(x, t) = F(x + at)$ means that along lines $x + at = \text{const}$, $u(x, t)$ is a constant. These lines with slope $dt/dx = -1/a$ form one family of parallel lines which are called characteristic lines (for reasons that will be apparent later). Any initial discontinuity will be carried unchanged along the characteristic as illustrated in Fig. 2.1. Since characteristics cannot intersect, discontinuities cannot develop spontaneously inside the domain; obviously, they can be introduced through the boundaries.

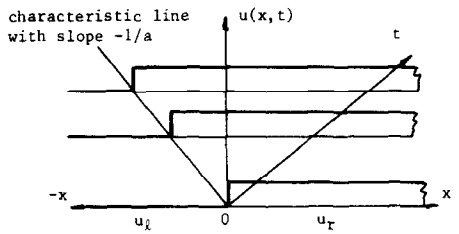

FIG. 2.1. Solution of Eq. (2.1) with an initial discontinuity

$$u(x, 0) = \begin{cases} u_l = 0, & x < 0, \\ u_r = 1, & x > 0. \end{cases}$$

Consider now the initial value problem

$$u_t + f(u)_x = 0, \qquad u(x,0) = F(x), \tag{2.6}$$

where $f(u) = u^2/2$; thus (2.6) can be written in the equivalent form

$$u_t + uu_x = 0. \tag{2.7}$$

The solution of (2.7) is constant along lines with slopes of $dt/dx = 1/u$. This one family of characteristic lines is a function of u and therefore the lines are straight since along them u is constant. Equation (2.7) differs from (2.1) mainly in that the characteristic lines need not be parallel; they can intersect or just diverge. In Fig. 2.2 we illustrate the intersection of characteristics. The initial conditions are $u(x,0) = F(x)$ as shown in the figure with $u_l = 1$ and $u_r = 0$ at the left and right, respectively, of segment AB and with a linear variation inside AB. The characteristics from the left of A will have slopes $1/u_l$ and those from the right of B, $1/u_r$, and in region AB they will have a fan-like pattern varying from $1/u_l$ to $1/u_r$. At point M they intersect, developing a discontinuity (the solution is not single valued), which will travel at a speed different from the speeds of both incoming characteristics. In fact this discontinuity or compressive shock travels with a speed s given by the jump conditions (Rankine–Hugoniot conditions in gas dynamics). It can be shown that the speed of the shock is constant and equal to

$$s = \frac{dx}{dt} = \frac{1}{2}\frac{f(u_r) - f(u_l)}{u_r - u_l} = \frac{(u_r + u_l)}{2}. \tag{2.8}$$

Thus, as indicated in Fig. 2.2, the shock moves along a line with slope $1/s = 2$.

In Fig. 2.3 we illustrate an example of diverging characteristics. The initial conditions are $u(x,0) = F(x)$ as shown in Fig. 2.3. Characteristics from the left and from the right diverge and, in zone OMB, the connection between the left and right states must be a fan-like pattern called a centered rarefaction wave; otherwise the solution for increasing time in sector OMB will be independent of the initial

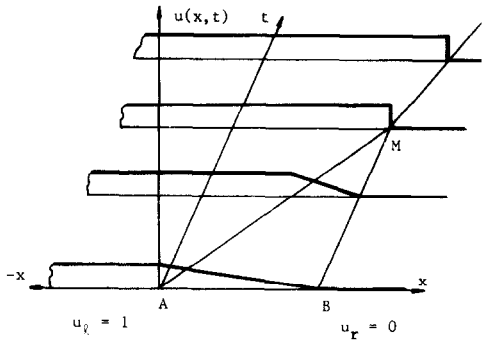

FIG. 2.2. The genesis of a discontinuity.

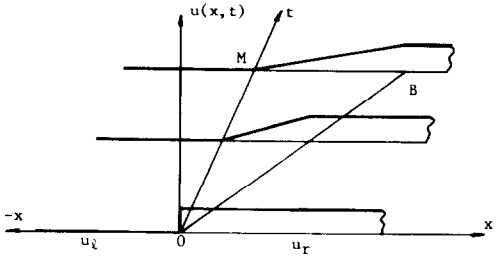

FIG. 2.3. Diverging characteristics.

conditions. We might think of connecting the left and right states by means of a rarefaction shock whose speed satisfies the jump conditions, but this situation does not exist in nature because it is forbidden by the entropy condition and therefore has to be ruled out. To this end we utilize the following criterion: the characteristics on either side of the discontinuity curve when continued in the direction of increasing time must intersect the line of discontinuity. This will be the case if

$$a(u_l) > s > a(u_r). \tag{2.9}$$

In the example illustrated in Fig. 2.2 condition (2.9) can be written as

$$\frac{1}{u_l} < \frac{1}{s} < \frac{1}{u_r}. \tag{2.10}$$

In gas dynamics this criterion is called the entropy condition because it is equivalent to requiring that the fluid which crosses the discontinuity suffer an increase in entropy (see Lax [7]).

We next introduce the Random Choice Method with a very simple example (see also Chorin and Marsden [4] or Concus and Proskurowski [5]). Consider the initial value problem given by Eq. (2.4) with initial conditions (2.2). The RCM provides with an approximation to the values of $u(x, t)$ at grid points $u_i^n = u(ih, nk)$, where i and n are integers and h and k the space and time steps, respectively. The RCM constructs the solution advancing the initial state forward in time by means of two fractional steps equal in length. We describe the first fractional step (the second is identical).

At time $t_n = nk$ the method approximates the solution $u(x, t_n)$ by a succession of constant states as illustrated in Fig. 2.4. Next, using as initial data the piecewise constant function, the theoretical solution of Eq. (2.4) is constructed, between $t_n = nk$ and $t_{n+1/2} = (n + 1/2)k$, by means of the solution of a succession of Riemann problems (one for each point $x_i = ih$). A Riemann problem is an initial value problem of the form

$$v_t - av_x = 0 \tag{2.11}$$

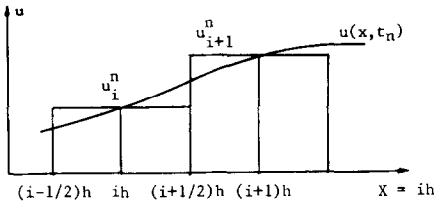

FIG. 2.4. Approximation of $u(x, t_n)$ by a piecewise constant function.

for $t > t_n$ with the initial conditions

$$\begin{aligned} v(x, t_n) &= u_i^n \qquad \text{for} \quad x < (i + 1/2)h \\ &= u_{i+1}^n \qquad \text{for} \quad x > (i + 1/2)h. \end{aligned} \tag{2.12}$$

In general there is a discontinuity in the initial data (2.12) which will propagate along the characteristic line with slope $1/a$. If there is a discontinuity for every grid point they will not interact provided the Courant–Friedrichs–Lewy (CFL) condition $k/h \leqslant 1/a$ is satisfied. In this case the solution of Eq. (2.4) at time $t_{n+1/2} = (n + 1/2)k$, with piecewise constant initial data at time $t_n = nk$, can be considered to be formed by the union of the solutions of each Riemann problem given by Eqs. (2.11) and (2.12).

Next the solution is sampled, by means of a random choice procedure, in the interval $[-h/2, h/2]$, for each point $(i + 1/2)h$, to obtain the value of the solution to be ascribed to each $u_{i+1/2}^{n+1/2}$. If $v(x, t)$ is the solution of Eqs. (2.11) and (2.12), then

$$u_{i+1/2}^{n+1/2} = v(P_i), \tag{2.13}$$

where P_i is a randomly chosen point with coordinates $[(i + 1/2 + 1/2\theta_{i+1/2})h, (n + 1/2)k]$, where $\theta_{i+1/2}$ is sampled at random from a distribution on the interval $[-1, 1]$.

With an identical procedure the solution is advanced from $t_{n+1/2}$ to t_{n+1} and the whole process is repeated for increasing time.

We consider in detail how the RCM works in the case of Eq. (2.4). Let us suppose that for a particular grid point $u_i^n < u_{i+1}^n$; therefore a discontinuity will travel along the characteristic line with slope $-1/a$. Using for convenience a local coordinate system with the origin in the point with coordinates $[(i + 1/2)h, nk]$ as shown in Fig. 2.5, the discontinuity will propagate through the points of coordinates $(0, 0)$ and $(ak/2, k/2)$. Accordingly the region of the xt plane to the right of the characteristic line will have the value corresponding to the solution at u_{i+1}^n, while everything to the left of it will have the value u_i^n; thus, theoretically $u_{i+1/2}^{n+1/2} = u_{i+1}^n$. In particular, after a time $T = 2nk/2$ the discontinuity will move to the left, from the local origin, the distance $X = -aT$.

In the RCM, according to expression (2.13) if the randomly chosen point P_i lies to the right of the characteristic $u_{i+1/2}^{n+1/2} = v_{i+1}^n$, which means that the solution will move $h/2$ to the left; however, if P_i lies to the left of the characteristic, $u_{i+1/2}^{n+1/2} = v_i^n$ and the

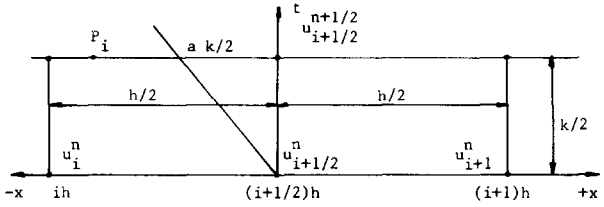

FIG. 2.5. Example of a Riemann problem and the RCM.

solution will move $h/2$ to the right. Since P_i is uniformly distributed, P_i lies to the right of the characteristic with probability $(h + ak)/(2h)$ and lies to the left with probability $(h - ak)/(2h)$. Thus, after $2n$ steps, the approximate value of u_i^n at $x = ih$ and $T = 2nk/2$ comes from the initial discontinuity at the location X_n where

$$X_n = \sum_{j=1}^{2n} \varepsilon_j \tag{2.14}$$

and ε_j are independent, identically distributed random variables with probability distribution

$$\text{Prob}[\varepsilon = -h/2] = \text{Prob}[P_i \text{ lies right charact.}] = (h + ak)/(2h), \tag{2.15}$$

$$\text{Prob}[\varepsilon = h/2] = \text{Prob}[P_i \text{ lies left charact.}] = (h - ak)/(2h). \tag{2.16}$$

The expectation and variance of ε are

$$E[\varepsilon] = \left(\frac{h + ak}{2h}\right)\left(-\frac{h}{2}\right) + \left(\frac{h - ak}{2h}\right)\frac{h}{2} = -\frac{ak}{2}, \tag{2.17}$$

$$\text{Var}[\varepsilon] = \tfrac{1}{4}(h^2 - a^2k^2). \tag{2.18}$$

Hence

$$E[X_n] = \sum_{j=1}^{2n} E(\varepsilon_j) = -nak = aT, \tag{2.19}$$

$$\text{Var}[X_n] = \sum_{j=1}^{2n} \text{Var}[\varepsilon_j] = \frac{k}{2}\left(\frac{1}{q^2} - a^2\right)T, \qquad \text{where} \quad q = \frac{k}{h}. \tag{2.20}$$

If q is kept constant $\text{Var}[X_n]$ tends to zero, for fixed T, as h tends to zero. We thus see that the approximate solution tends to the theoretical solution as h is diminished, proving the convergence of the RCM.

We note that in the event that $q = k/h = 1/a$, we have $\text{Var}[X_n] = 0$; therefore, in this case the computed and theoretical solutions coincide for any values of k and h which satisfy the CFL condition.

In the simple example provided by Eq. (2.4) the solution of the Riemann problem is trivial. For more complex problems the success of the RCM depends on the

possibility of solving the Riemann problem exactly and inexpensively and on the sampling technique. Chorin [2, 3] has developed the appropriate sampling strategies which are decisive for the success of the RCM (see further details in the Appendix).

3. A Pair of Conservation Laws and the Random Choice Method

In this section we introduce the quasi-linear hyperbolic system of conservation laws of long waves in shallow water and its gas dynamic analogy and solution by the RCM.

The shallow water equations can be written (see Stoker [12]) as

$$u_t + uu_x + g\eta_x = 0, \tag{3.1}$$

$$\eta_t + [u(\eta + h)]_x = 0, \tag{3.2}$$

where u is the water velocity, h is the depth of the undisturbed water, η is the free surface elevation, g is the gravity, and x and t are the space and time coordinates, as shown in Fig. 3.1.

In order to make use of the gas dynamic analogy we introduce the quantities

$$\bar{\rho} = \rho(\eta + h), \tag{3.3}$$

where $\bar{\rho}$ is the "gas" density and ρ is the water density, and

$$\bar{P} = \int_{-h}^{\eta} p\, dy = \int_{-h}^{\eta} g\rho(\eta - y)\, dy = g\bar{\rho}^2/(2\rho). \tag{3.4}$$

From Eq. (3.4) the relation between pressure and density for this particular "γ law gas" is obtained:

$$\bar{P} = A\bar{\rho}^{\gamma}, \qquad \text{where} \quad A = g/2\rho \quad \text{and} \quad \gamma = 2. \tag{3.5}$$

Taking into account Eqs. (3.4) and (3.5) and the fact that $\eta = \eta(x, t)$ and $h = h(x)$, system (3.1)–(3.2) becomes

$$u_t + uu_x + (1/\rho)\bar{P}_x - gh_x = 0, \tag{3.6}$$

$$\bar{\rho}_t + (\bar{\rho}u)_x = 0. \tag{3.7}$$

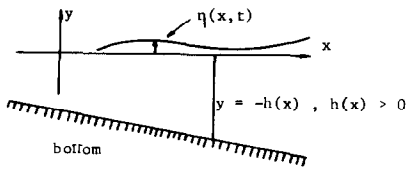

FIG. 3.1. Coordinate system for the shallow water equations.

The shallow water equations (3.6) and (3.7) with $h_x = 0$ are identical with the equations of isoentropic flow of a perfect gas with constant specific heat. In this analogy the depth of the water plays the role of the density of the gas.

The sound speed $c = (dp/d\rho)^{1/2}$ of gas dynamics will be

$$\bar{c} = (g\bar{\rho}/\rho)^{1/2} = (g(\eta + h))^{1/2}. \tag{3.8}$$

This quantity $\bar{c}$ represents the speed of propagation of small disturbances, relative to the fluid velocity (see details in Stoker [12]).

Next we introduce the concept of Riemann Invariants, which, as we shall see, are constant quantities along characteristic lines. To this end we rewrite system (3.6)–(3.7) with the help of Eq. (3.8) (see Stoker [12] for details).

$$u_t + uu_x + 2\bar{c}\bar{c}_x - H_x = 0, \tag{3.9}$$

$$2\bar{c}_t + 2u\bar{c}_x + \bar{c}u_x = 0, \tag{3.10}$$

where $H = gh$. Supposing $H_x = m = \text{const}$ and adding and substracting Eqs. (3.9) and (3.10), respectively, we obtain a system which can be written

$$\left\{\frac{\partial}{\partial t} + (u + \bar{c})\frac{\partial}{\partial x}\right\}(u + 2\bar{c} - mt) = 0, \tag{3.11}$$

$$\left\{\frac{\partial}{\partial t} + (u - \bar{c})\frac{\partial}{\partial x}\right\}(u - 2\bar{c} - mt) = 0. \tag{3.12}$$

Equations (3.11) and (3.12) can be written

$$\frac{DJ_+}{Dt} = 0 \qquad \text{provided} \quad \frac{dx}{dt} = u + \bar{c}, \tag{3.13}$$

$$\frac{DJ_-}{Dt} = 0 \qquad \text{provided} \quad \frac{dx}{dt} = u - \bar{c}. \tag{3.14}$$

Equations (3.13) and (3.14) indicate that the quantities J_+ and J_- are constant along lines whose slopes are $dx/dt = u \pm \bar{c}$, respectively. These lines are called characteristic lines and $J_\pm$ Riemann Invariants. In isoentropic gas dynamic flow the Riemann Invariants are given by $J_\pm = u \pm (2/(\gamma - 1))c$. Hereafter we shall suppose that $H_x = 0$. In this way the analogy between gas dynamics and shallow water is complete.

According to Eqs. (3.13) and (3.14) we have two families of characteristics: the C_+ and C_-, along which J_+ and J_- are constant, respectively. If characteristics of the same family intersect a discontinuity is formed and the theory ceases to be valid; therefore a broader class of solutions, called generalized solutions (weak solutions),

must be considered. To this end we again write Eqs. (3.6) and (3.7) as a pair of conservation laws (for simplicity we drop the bars over the variables ρ and P):

$$\rho_t + m_x = 0, \tag{3.15}$$

$$m_t + (m^2/\rho + P)_x = 0, \qquad \text{where } m = \rho u \text{ and } P = P(\rho) = A\rho^{\gamma}. \tag{3.16}$$

Following the notation of Section 2 we can write system (3.15)–(3.16) as

$$W_t + F(W)_x = 0, \qquad W = [\rho, m]^T \qquad \text{and} \qquad F(W) = [f(W), g(W)]^T. \tag{3.17}$$

Differentiation of Eq. (3.17) gives the equivalent system

$$W_t + A(W)W_x = 0, \qquad \text{where} \quad A(W) = \begin{bmatrix} 0 & f_m \\ g_\rho & g_m \end{bmatrix}. \tag{3.18}$$

The eigenvalues of $A(W)$ are $\lambda_k = u \pm c$ (the slope of the characteristic lines).

Certainly a generalized (weak) solution of the system of conservation laws (3.18) must satisfy the Rankine–Hugoniot conditions across every curve of discontinuity, i.e.,

$$s[W] = [F], \tag{3.19}$$

where s is the speed of propagation of the discontinuity. For the single conservation law presented in Section 2 the entropy condition requires that the characteristics on either side of a discontinuity run into the line of discontinuity, which is the case if the characteristic speed on the left is greater, on the right less, than s:

$$\lambda(u_l) > s > \lambda(u_r), \tag{3.20}$$

where $\lambda = a(u_l)$ is the eigenvalue of Eq. (2.10). The entropy condition for systems requires that for some index k, $1 < k < n$ (where n are the eigenvalues of matrix $A(W)$ of Eq. (3.18)),

$$\lambda_k(u_l) > s > \lambda_k(u_r) \tag{3.21}$$

while

$$\lambda_{k-1}(u_l) < s < \lambda_{k+1}(u_r). \tag{3.22}$$

These inequalities assert that k characteristics inpinge the line of discontinuity from the left and $n - k + 1$ from the right, a total of $n + 1$ (see Lax [7]).

Next we study the Riemann problem for the shallow water equations (3.17). Let us consider the following initial data for system (3.17) (illustrated in Figs. 3.2a and b):

$$W(x, 0) = \begin{cases} S_l = (u_l, \rho_l) & \text{for} \quad x < 0, \\ S_r = (u_r, \rho_r) & \text{for} \quad x > 0. \end{cases} \tag{3.23}$$

The solution at later times might look like Figs. 3.2a and b. S_l and S_r indicate left and right initial states, respectively. There are also two other possible solutions depending on the initial conditions: two shocks in opposite directions and two rarefaction waves in opposite directions. These solutions are taken into account by the RCM. In Fig. 3.2a, for instance, we have a right shock wave and a left centered rarefaction wave; the region between them is a steady state region termed S_*; in the case of a gas the line with slope u_*^{-1} indicates the position of the slip line, but in fluids, as there is no slip line, it just indicates the slope of the velocity u_*.

We might think of connecting the S_* state and the S_l state (see Fig. 3.2a) by a "rarefaction" or depression shock satisfying the jump conditions. This situation is forbidden by the entropy condition for systems of conservation laws. This condition merits a short discussion for the shallow water equations. As was noted earlier, in Section 1, the shallow water theory prescribes a loss of energy at the jump; i.e., the particles which cross the jump cannot gain energy (see Stoker [12]). This energy condition requires that the particles always move across the shock from a region of lower total depth to a region of higher total depth. In other words, only "compressive" hydraulic jumps are physically correct. Thus the energy condition, which rules out the rarefaction jump, is the analogy of the entropy condition in gas dynamics (in fact a loss of energy through an irreversible process implies an increase in entropy). In Fig. 3.2a the characteristics of J_+ family originating at both sides of the initial discontinuity, on the X axis, intersect producing the right shock. This shock separates two constant state regions S_* and S_r. The J_- characteristics constitute a family of straight parallel lines in S_* and S_r, whose slopes change in crossing the shock.

Next we consider the solution of the Riemann problem given by Eqs. (3.17) and (3.23). We use a modified version of the Chorin–Godunov iterative method (the Godunov method can be found in Richtmyer and Morton [9]) utilized by Chorin in

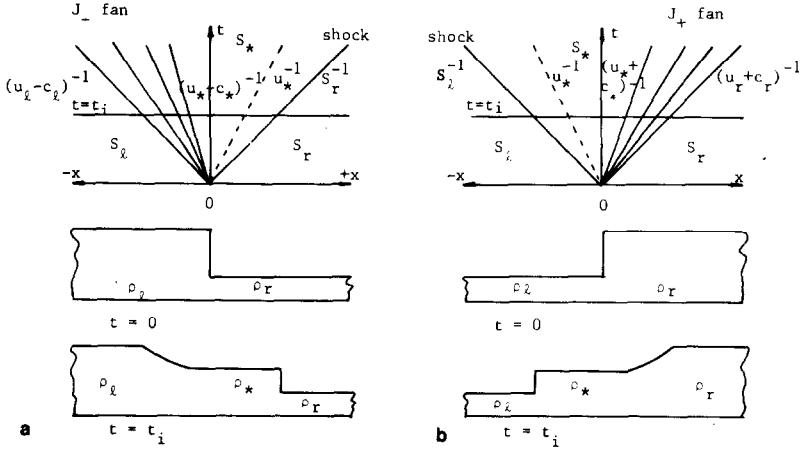

FIG. 3.2. (a) The Riemann problem for $\rho_l > \rho_r$: right shock and $\rho_l > \rho_* > \rho_r$. (b) The Riemann problem for $\rho_l < \rho_r$: left shock and $\rho_l < \rho_* < \rho_r$.

the solution of gas dynamics problems (see Chorin [2]). By this method we first evaluate P_* in the state S_* (for convenience we use the variable P instead of ρ). We define the quantity

$$M_l = \frac{P_l - P_*}{u_l - u_*}. \tag{3.24}$$

If the left wave is a shock it can be shown (see the Appendix), that

$$M_l = \rho_l(u_l - s_l) = \rho_*(u_* - s_l). \tag{3.25}$$

In the same way we define

$$M_r = \frac{P_r - P_*}{u_r - u_*}. \tag{3.26}$$

If the right wave is a shock then

$$M_r = -\rho_r(u_r - s_r) = \rho_*(u_* - s_r). \tag{3.27}$$

In either of the two cases, expression (3.24) or expression (3.25) for M_l, and (3.26) or (3.27) for M_r, we obtain

$$M_r = (\rho_r P_r)^{1/2} F(X), \tag{3.28}$$

$$M_l = (\rho_l P_l)^{1/2} F(X), \tag{3.29}$$

where

$$F(X) = \frac{(X-1)^{1/2}}{(1-(1/X)^{1/2})^{1/2}} \qquad \text{for} \quad X > 1$$

$$= \frac{1-x}{2.83(1-x^{1/4})} \qquad \text{for} \quad X < 1$$

and

$$X = P_*/P_r.$$

From Eqs. (3.24) and (3.26) we obtain

$$P_* = \frac{u_l - u_r + P_r/M_r + P_l/M_l}{1/M_l + 1/M_r}. \tag{3.30}$$

Expressions (3.28), (3.29), and (3.30) constitute a closed system of equations for which a real solution exists. The iteration process starts with an initial guess for P_*^0 (or M_l^0 and M_r^0). Following the idea of Chorin we use as an initial guess $P_*^0 = (P_* + P_l)/2$ (more details on the iteration process can be found in Chorin [2] and

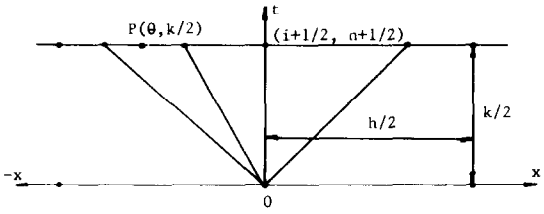

FIG. 3.3. Sampling of the Riemann problem in case A.

Sod [10]). With the values of P_*, M_l, and M_r, u_* may be obtained by means of Eqs.. (3.24) and (3.26):

$$u_* = \frac{P_l - P_r + M_l u_l + M_r u_r}{M_l + M_r}. \tag{3.31}$$

Next we discuss the implementation of the RCM for the shallow water equations. The fluid is initially in the state given by Eq. (3.23). The Riemann solution obtained with the iteration just described is sampled at $t = k/2$ and $X = \theta h/2$. We may distinguish two cases.

(A) If $P_* > P_r$, the right wave is a shock and P $(\theta h, k/2)$ may lie within four possible segments (illustrated in Figs. 3.2a and 3.3).

(B) If $P_* < P_r$, the right wave is a rarefaction wave and P $(\theta h, k/2)$ may lie within four possible segments.

Case A. The velocity of the right shock S_r is given by Eq. (3.27). If the sample point P lies to the right of the shock line S_*^{-1}, we have $P = P_r$ $(\rho = \rho_r)$ and $u = u_r$. If P lies to the left of the shock, $P = P_*$ $(\rho = \rho_*)$ and $u = u_*$. If P lies to the left of the left rarefaction wave, $P = P_l$ $(\rho = \rho_l)$ and $u = u_l$. If P lies inside the left rarefaction wave, then $u - c = 2\theta h/k$; the constancy of the J_l Riemann invariant and the γ law $p = A\rho^\gamma$, together with $c = (\gamma P/\rho)^{1/2}$, gives u and P $(\rho = \rho(P))$.

Case B is quite similar to Case A and is not described.

The treatment of boundary conditions is fully documented in the work of Chorin [2] and therefore is not presented here.

4. NUMERICAL RESULTS

In this section we present some numerical results of the Random Choice Method applied to the problem of the breaking of a dam and a comparison with the results obtained by Stoker [12] and Ré [8].

The problem of the breaking of a dam is illustrated in Fig. 4.1. At time $t = 0$ the dam is suddenly destroyed and the problem is to determine the subsequent motion of the water for all X and t. The initial conditions (see Stoker [12] or Ré [8]) are the

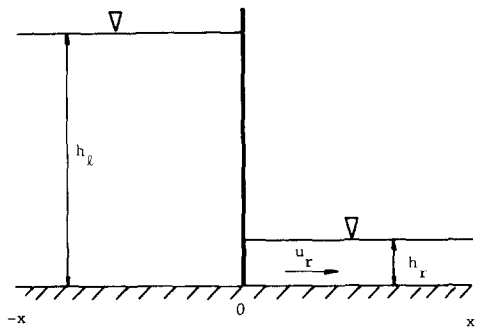

FIG. 4.1. The breaking of a dam.

upstream and downstream heights of the water and the velocity downstream (the velocity upstream is determined by the continuity condition). In our example these are

$$W(x, 0) = \begin{cases} S_l = (h_l = 10.8 \text{ m}, u_l = 0.2667 \text{ m/sec}), \\ S_r = (h_r = 1.8 \text{ m}, \ u_r = 1.6 \text{ m/sec}). \end{cases} \tag{4.1}$$

The situation at later times is illustrated in Fig. 3.2a: a shock is moving to the right and a depression wave is moving to the left, separated by a constant state.

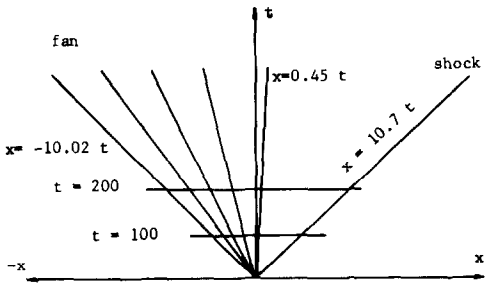

FIG. 4.2a. The Riemann problem solution (data from Stoker [12]).

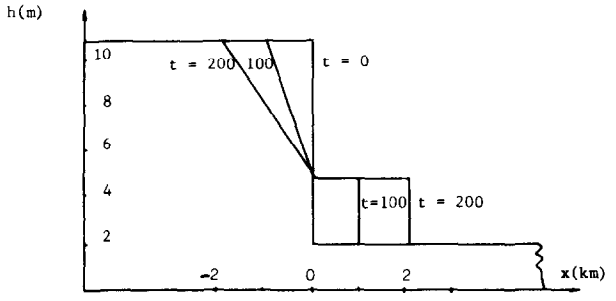

FIG. 4.2b. Height of water for different times (data from Stoker [12]).

In Figs. 4.2a and b, 4.3, and 4.4, we present the numerical solutions obtained by Stoker [12] and Ré [8] and with the RCM, respectively.

Stoker's solution is the theoretical solution and therefore we take it as our standard of reference. The solution obtained by Ré (Fig. 4.3) shows a distortion in the amplitude and speed of propagation of the shock and the absence of a constant state behind the shock. This behaviour is due solely to the dissipative character of the method utilized (for small values of time the resistance and slope terms are negligible; see Stoker [12]).

The solution by the Random Choice Method in Fig. 4.4 shows that the shock wave and the depression wave have been computed with almost infinite resolution. Because

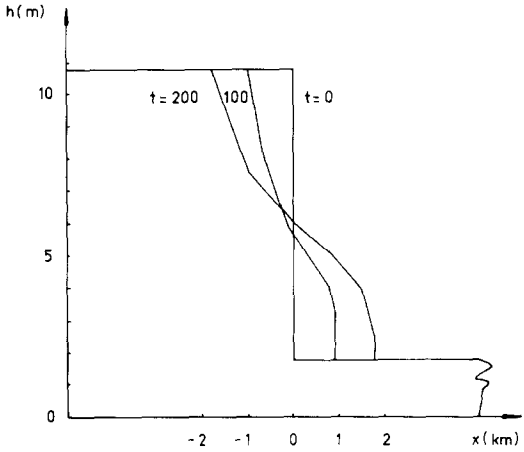

FIG. 4.3. Height of water for different times (data from Ré [8]).

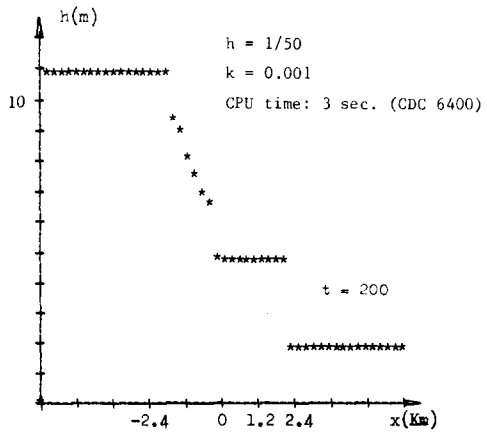

FIG. 4.4. Height of water after 16 time steps obtained with the Random Choice Method.

of the random character of the method the locations of the shock and the depression wave are not exact. However, on the average, their locations are exact. The constant state is represented exactly. Although the depression wave is not smooth it is very close to the theoretical solution. It is then possible to observe the accuracy of the RCM method by comparing Figs. 4.4 and 4.2b; in fact, both solutions should give very close results since Stoker's is in essence the same as the Godunov iterative scheme, the only difference being its deterministic character.

In Table I we present an example of the influence of the sampling technique on the quality of the solution when the following strategies are used: (a) only one value of θ is picked for each time level, and (b) only one value of θ is picked for each time step but the θ_i are picked according to the modified sequence outlined in the Appendix. The two experiments are compared when n is a multiple of m_2 and thus the solution in case b is likely to be at its highest accuracy.

TABLE I

	h	
x	Case a	Case b
0.2449	10.8000	10.8000
0.2653	10.8000	10.8000
0.2857	10.8000	10.8000
0.3061	10.8000	10.8000
0.3265	10.8000	10.7236
0.3469	10.5648	9.3177
0.3673	9.0179	8.6082
0.3877	8.4341	8.1966
0.4081	8.2866	7.3805
0.4285	8.2356	7.3781
0.4489	7.2731	6.5995
0.4693	6.6384	6.1101
0.4898	4.7132	5.7670
0.5102	4.7132	4.7132
0.5306	4.7132	4.7132
0.5510	4.7132	4.7132
0.5714	4.7132	4.7132
0.5918	4.7132	4.7132
0.6122	4.7132	4.7132
0.6326	4.7132	4.7132
0.6530	4.7132	4.7132
0.6734	4.7132	4.7135
0.6938	4.7132	1.8000
0.7142	1.8000	1.8000
0.7346	1.8000	1.8000
0.7551	1.8000	1.8000
0.7755	1.8000	1.8000

Note. $h = 1/50$, $k = 0.0005$, $n = 33$, $m_1 = 3$, $m_2 = 11$.

TABLE II

x	h
0.2449	10.8000
0.2653	10.8000
0.2857	4.9345
0.3061	4.9342
0.3265	4.9392
0.3469	4.9319
0.3673	4.9309
0.3877	4.9305
0.4081	4.9289
0.4285	4.9286
0.4489	4.9270
0.4693	4.9267
0.4898	4.9250
0.5102	4.9246
0.5306	4.9242
0.5510	4.9235
0.5714	4.9221
0.5918	4.9211
0.6122	4.9198
0.6326	4.9195
0.6530	4.9174
0.6734	4.9173
0.6938	4.9169
0.7142	4.9156
0.7346	1.8000
0.7551	1.8000
0.7755	1.8000

Note. $h = 1/50$, $k = 1$, $n = 11$, $m_1 = 3$, $m_2 = 11$.

Although the RCM is unconditionally stable, if the CFL condition is violated, the consistency is lost. This is sown in Table II, where the CFL condition is grossly violated ($k \simeq 100\, k_{\text{crit}}$): the depression zone is transformed into a fake constant state (compare with Table I, case b).

In Table III we show the effect of the space step size on the quality of the solution ($h = 1/20$). Comparison with corresponding values in Table I shows very good agreement, in spite of the coarseness of the grid utilized. A coarse mesh is most likely to affect the solution in the depression zone.

5. Conclusions

We have introduced a random choice method (RCM) for the numerical solution of the shallow water equations in the light of the analogy with gas dynamics.

TABLE III

x	h
0.2105	10.8000
0.2631	10.8000
0.3157	10.8000
0.3684	9.7411
0.4210	8.2409
0.4736	7.2316
0.5263	4.7132
0.5789	4.7132
0.6315	4.7132
0.6842	4.7132
0.7368	1.8000
0.7894	1.8000
0.8421	1.8000

Note. $h = 1/20$, $k = 0.0005$, $n = 33$, $m_1 = 3$, $m_2 = 11$.

The method is particularly appropriate for the treatment of discontinuities. It is unconditionally stable and has almost infinite resolution. It can easily be extended to two dimensional rectangular coordinates using splitting techniques.

It is planned to use the present method for the solution of high Reynolds viscous flows in conjunction with appropriate boundary layer approximations.

APPENDIX

Shock Relations

In this section we present an analysis of the shock relations for the case of a right shock illustrated in Fig. A.1.

In the figure u_* and u_r are the absolute velocities, S is the speed of the shock relative to the downstream velocity u_r, and $S + u_r$ is the absolute velocity of the shock. Figure A.2 illustrates the relative velocities with reference to a frame moving with the absolute velocity of the shock.

Conservation of mass $(S + u_r)[\rho] = [\rho u]$ becomes

$$\rho_*(u_* - S - u_r) = -\rho_r S. \tag{A.1}$$

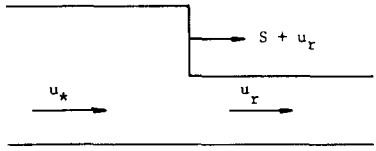

FIG. A.1. Right shock wave, absolute velocities.

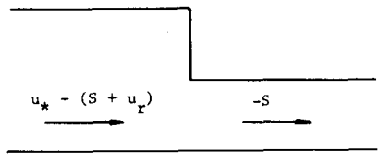

FIG. A.2. Right shock wave, relative velocities.

Conservation of momentum $(S + u_r)[\rho u] = [\rho u^2 + p]$ becomes

$$-\rho_r S(u_* - u_r) = P_r - P_*. \tag{A.2}$$

From Eqs. (A.1) and (A.2) we obtain

$$u_* - u_r = \frac{((p_* - p_r)(\rho_* - \rho_r))^{1/2}}{(\rho_* \rho_r)^{1/2}}. \tag{A.3}$$

The conservation of momentum can also be written as

$$M_r = -\frac{P_r - P_*}{u_r - u_*}. \tag{A.4}$$

Replacing Eq. (A.3) in (A.4) and after some algebraic manipulations we obtain

$$M_r = -\frac{(P_r \rho_r)^{1/2}(X-1)^{1/2}}{(1-(1/X)^{1/2})^{1/2}}, \tag{A.5}$$

where $X = P_*/P_r$.

Rarefaction Wave

Here we present an analysis of the rarefaction wave relations for the case of a right rarefaction wave as illustrated in Fig. A.3.

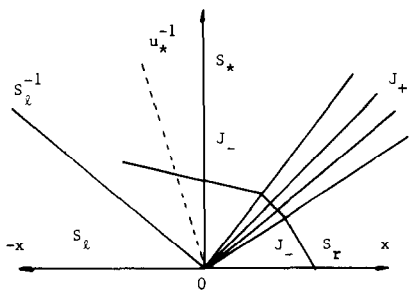

FIG. A.3. Right rarefaction wave.

Let us define the quantity

$$M_r = \frac{P_r - P_*}{u_r - u_*}. \tag{A.6}$$

With the help of the J_- characteristic we obtain

$$u_r - u_* = 2(c_r - c_*). \tag{A.7}$$

Replacing Eq. (A.7) in (A.6), using Eqs. (3.5) and (3.8), and after some algebra we obtain

$$M_r = \frac{(P_r \rho_r)^{1/2}(1 - x)}{2.83(1 - x^{1/4})}, \qquad \text{where} \quad X = P_*/P_r. \tag{A.8}$$

The Sampling Technique

The sampling strategies crucial for the success of the RCM method were developed by Chorin [2, 3].

The magnitude of the random variable ε (see Section 2) depends on the choices of θ. The strategy of picking a new value of θ, for each space step and each time step, is disastrous in practice because of the possible generation of spurious constant states. Chorin introduced the idea of picking only one θ per time step, thus greatly improving the method. In the example shown in Section 2, the standard deviation of ε, which measures its magnitude, is $n^{1/2}h/2\{(1 - aq)\,(1 + aq)\}^{1/2} = O(n^{1/2}h)$.

For further reducing the variance of the solution Chorin proposed the following strategy: the interval $[-\frac{1}{2}, \frac{1}{2}]$ is divided into m_2 subintervals $m_2 < n$, and θ_1 is picked at random in the first subinterval, θ_2 in the second subinterval, $\theta_{m_{2+1}}$ in the first subinterval, etc. This subinterval ordering is obtained through the formula $n_{i+1} = (m + n_i) \bmod m_2$, where $m_1, m_2, m_1 < m_2$ are prime integers and n_0 given, $n_0 < m_2$. It is clear that since only one θ_i is picked per time step, after $n = m_2$ steps m_2 values of θ have been picked and each one in a different subinterval. In this way the θ_i reach approximate equidistribution over $[-\frac{1}{2}, \frac{1}{2}]$ at a faster rate. If this strategy is used in the example of Section 2 and n is multiple of m_2, the standard deviation of ε is of order $O(h(n/m_2)^{1/2})$, thus showing the advantage of this last technique over the preceding one.

ACKNOWLEDGMENTS

The authors are deeply indebted to Alexander Chorin for his many illuminating discussions on the Random Choice Method. His pioneering work is fundamental to the results presented here. The authors would also like to thank C. Fenimore, V. Proskurowski, A. Shestakov, and G. Sod for helpful discussions and comments.

The first author gratefully aknowledges a scholarship granted by IBM Argentina..

REFERENCES

1. M. B. ABBOTT, "An Introduction to the Method of Characteristics," Elsevier, Amsterdam, 1966.
2. A. J. CHORIN, Random choice solutions of hyperbolic systems, *J. Comput. Phys.* **22** (1976), 517–533.
3. A. J. CHORIN, Random choice methods with application to reacting gas flow, *J. Comput. Phys.* **25** (1977), 253–272.
4. A. J. CHORIN AND J. E. MARSDEN, "Mathematical Introduction to Fluid Mechanics," Springer-Verlag Graduate Texts in Mathematics, Springer-Verlag, New York/Berlin, 1979.
5. P. CONCUS AND W. PROSKUROWSKI, "Numerical Solution of a Non-linear Hyperbolic Equation by the Random Choice Method," Lawrence Berkeley Lab. Report 6487 (1977).
6. R. COURANT AND K. O. FRIEDRICHS, "Supersonic Flow and Shock Waves," Interscience, New York, 1948.
7. P. D. LAX, "Hyperbolic Systems of Conservation Laws and the Mathematical Theory of Shock Waves," Appl. Math. Series, Vol. 11, SIAM, Philadelphia, 1973.
8. R. RÉ, Etude du lacher instantané d'une retenue d'eau dans un canal par la methode graphique, *La Houille Blanche* **3** (1946), 181–187.
9. R.D. RICHTMYER AND K. W. MORTON. "Finite Difference Methods for Initial Value Problems," Interscience, New York, 1967.
10. G. SOD, "A Survey of Numerical Methods for Compressible Fluids," ERDA Report COO-3077-145, Courant Inst. Math. Sciences, New York University, 1977.
11. G. SOD, "A Numerical Study of a Converging Cylindrical Shock," UCRL 79517, Lawrence Livermore Lab., University of California, 1977.
12. J. J. STOKER, The formation of breakers and bores, *Comm. Pure Appl. Math.* **1** (1948).
13. T. STRELKOFF, D. SCHAMBER, AND K. KATOPODES, Comparative analysis of routing techniques for the flood wave from a ruptured dam, *in* "Proceedings, Dam-Break Flood Routing Model Workshop, Hydrology Committee of the W.R.C. USA, 1978."